Study of the Formation of the Layered Double Hydroxide [Zn−Cr−Cl]

Hervé Roussel,[†] Valérie Briois,*[,†] Erik Elkaim,[†] André de Roy,[‡] Jean-Pierre Besse,[‡] and Jean-Pierre Jolivet[§]

Laboratoire pour l'Utilisation du Rayonnement Electromagnétique, Bât 209 D Centre, Universitaire Paris-Sud, BP34, 91898 Orsay Cedex, France, Laboratoire des Matériaux Inorganiques, CNRS UPRES-A 6002, Université Blaise Pascal, 63177 Aubiere Cedex, France, and Chimie de la Matière Condensée, CNRS UMR 7574, Université Pierre et Marie Curie, 4 place Jussieu, 75252 PARIS Cedex 05, France

Received April 17, 2000. Revised Manuscript Received September 27, 2000

The synthesis of the layered double hydroxide (LDH) [Zn−Cr−Cl], well-known for its ability to be synthesized only with the ratio Zn:Cr = 2:1, has been followed by UV−visible and extended X-ray absorption fine structure (EXAFS) spectroscopy in order to understand the mechanisms of its formation. The UV−visible spectrum reveals first the hydrolysis of the Cr(III) monomer units, favored by the acidity conditions, followed by the formation of trimer and tetramer species. The EXAFS experiments at the Cr K-edge confirm the formation of the oligomeric species before the LDH signature. At the Zn K-edge, the results show that hexaaquozinc(II) complexes are present before the formation of the LDH phase. During LDH synthesis, oligomeric chromium(III) species and hexaaquozinc(II) complexes coexist in solution with the LDH solid. A structural pathway based on direct condensation of hexaaquozinc(II) complexes with deprotonated Cr(III) monomeric species is proposed to explain the formation of LDH solid with ratio Zn:Cr = 2. The structural pathway strongly supports the concept of cationic order in the [Zn−Cr−Cl] LDH sheets suggested by several authors but not demonstrated until now. Nevertheless we cannot exclude some faults during condensation as incorporation of a few oligomers such as dimers, trimers, and planar tetramers, but this should be very exceptional since the condensation of chromium oligomers with zinc monomers would lead to an LDH solid with a Zn:Cr ratio less than 2.

Introduction

Layered double hydroxides (LDH) are constituted by infinite sheets of brucite-type material charged positively, where trivalent cations have replaced a fraction x of divalent cations in octahedral coordination. The general formula for these compounds is $[M_{1-x}^{II}M_x^{III}(OH)_2]^{+}\cdot A_x^{-}\cdot nH_2O$, abbreviated hereafter as $[M^{II}-M^{III}-A]$, where M^{II} and M^{III} are divalent and trivalent cations and A represents interlamellar anions that restore the electroneutrality of the structure. As anions are weakly bonded to the host structure, LDHs are known as good anionic exchangers.[1−2] The LDHs compounds are also widely used in the industrial domain, especially for their catalytic properties.[3−8]

The [Zn−Cr−Cl] LDH is well-known for its ability to be synthesized only with $x = 0.33$, i.e., a ratio Zn:Cr = 2:1,[6,9−12] whatever the nominal proportion of zinc and chromium in the starting solution. To explain this phenomenon, Gutmann and Muller[12] proposed the insertion of monomer Cr(III) units into the hydroxide layers within the sheets, according to the ideal model of cationic arrangement for $x = 0.33$ given by Hofmeister and Platen[13] and de Roy et al.,[11] where a trivalent cation is surrounded by six divalent cations, and a divalent cation is surrounded by three divalent and three trivalent cations. The titration curve of solutions containing Zn(II) and Cr(III) chlorides by NaOH reported by Boclair and Braterman[9] is characterized by a process of only one step. Authors concluded consequently that there is direct formation of the LDH. On the other hand, titrations of solutions containing cations M(II) and M(III) other than Cr(III),[14] evidenced first the formation of the M(III) hydroxide, followed by the LDH appearance. As titrations of solutions containing M(II)−Cr(III)

* To whom correspondence should be adressed. E-mail briois@lure.u-psud.fr.
† Université Paris-Sud.
‡ Université Blaise Pascal.
§ Université Pierre et Marie Curie.

(1) Miyata, S. *Clays Clay Miner.* **1983**, *31*, 3050.
(2) Miyata, S. *Kagaku Gijutsushi Mol.* **1977**, *15*, 32.
(3) Vaccari, A. *Catal. Today* **1998**, *41*, 53.
(4) Cavani, F.; Trifiro, F.; Vaccari, A. *Catal. Today* **1991**, *11*, 173.
(5) Pinnavaia, T. J. *Science* **1983**, *220*, 365.
(6) Martin, K. J.; Pinnavaia, T. J. *J. Am. Chem. Soc.* **1986**, *108*, 541.
(7) Reichle, W. T. *J. Catal.* **1985**, *94*, 547.
(8) Reichle, W. T.; Kang, S. Y.; Everhardt, D. S. *J. Catal.* **1986**, *101*, 352.
(9) Boclair, J. W.; Braterman, P. S. *Chem. Mater.* **1998**, *10*, 2050.
(10) Boehm, H. P.; Steinle, J.; Viewger, C. *Angew. Chem., Int. Ed. Engl.* **1977**, *16*, 265.
(11) de Roy, A.; Forano, C.; El Malki, K.; Besse, J. P. In *Synthesis of Microporous Materials*; Occelli, M. L., Robson, H. E., Eds.; Van Nostrand Reinhold: New York, 1992; Vol. II, p 108.
(12) Gutmann, N.; Muller, B. *J. Solid State Chem.* **1996**, *122*, 214.
(13) Hofmeister, W.; Platen, H. V. *Cryst. Rev.* **1992**, *3*, 3.
(14) Boclair, J. W.; Braterman, P. S. *Chem. Mater.* **1999**, *11*, 298.

10.1021/cm001066w CCC: $20.00
Published on Web 01/05/2001

cations have also shown a one-step process,[15] the Cr(III) seems to play a key role in the LDH formation.

To understand more precisely the role of Cr(III) in [Zn−Cr−Cl] formation and to explain the constant ratio Zn:Cr = 2:1, we have undertaken to follow the formation of [Zn−Cr−Cl] during its synthesis by UV−visible and EXAFS spectroscopy at both cation K-edges. The UV−visible technique gives information concerning the condensation degree of Cr(III),[16] since Cr(III) is well-known to form polycations[17] in aqueous solutions. EXAFS experiments performed simultaneously at both cation K-edges allow us to investigate local environment around each cation at the same stage of the formation of the LDH.

Experimental Section

Synthesis. The [Zn−Cr−Cl] LDH was prepared by coprecipitation of 18 mL of a mixed solution of $ZnCl_2$ and $CrCl_3$, both at concentration 1 M, in a ratio Zn:Cr = 2:1 and at controlled pH. The premixed solution of salts was added at 0.6 mL·h^{-1} at a constant flow rate with a syringe pump, in a reactor containing 500 mL of decarbonated water. The pH was maintained during synthesis at 5.0 by the addition of a 1 M NaOH solution through another syringe pump regulated by an electronic system. The complete addition of the solution of metallic salts took 30 h. After several washes in distilled decarbonated water, products were air-dried at room temperature and characterized by X-ray diffraction (XRD) to verify the purity of the so-obtained LDH phase.

Measurements and Data Analysis. To describe the system at different stages during the synthesis of LDH, a small amount of solutions (about 3 mL) was regularly extracted from the reactor (every 30 min), and characterized by UV−visible and EXAFS techniques. Each solution was referenced to the volume of mixed salts solution added as of the time at which it was collected in the reactor. For some of the samples, preparative centrifugation (at 15 300 rpm for 10 h) was used in order to isolate the solid LDH phase from possible ionic species remaining in solution. The supernatant solutions so obtained were also characterized by UV−visible and EXAFS spectroscopy.

UV−Visible Spectroscopy. UV−Visible spectra were recorded on a Shimadzu UV-2101PC, in the range 350−800 nm with a 0.5 nm step. We report as sample signature the couple of values (λ_1, λ_2, α) corresponding to the wavelengths (in nanometers) of the two absorbance maxima and their absorbance ratio, noted α. The validity of the calibration of the UV spectrometer was obtained by recording the spectrum of a Cr(III) solution 0.01 M prepared from $CrCl_3 \cdot 6H_2O$ salt and 2 years aged, which contains mainly hexaaquochromium(III) complexes. The parameters obtained for this solution ($\lambda_1 = 409$ nm, $\lambda_2 = 576$ nm, $\alpha = 1.17$) were quite similar to the ones obtained in the literature by Stünzi and Marty[16] [see Table 2 for the $Cr(H_2O)_6^{3+}$ monomer].

EXAFS. The local order around Cr and Zn cations was investigated at the same time, on the same sample separated into two parts in order to be characterized on two different experimental setups. Spectra at the Cr and Zn K-edges were recorded on the experimental stations D42 and D44 (LURE-DCI storage ring, Orsay, France), respectively. Due to the low concentrations of the cations (from $\approx 2 \times 10^{-3}$ to 10^{-2} M for Cr), fluorescence mode was used as detection. A Si/Li mono-element Eurysis solid-state detector and a Ge 7-elements Canberra solid-state detector were used on D44 and D42, respectively. A Si(111) double-crystal monochromator was used for energy selection at both edges. Harmonic rejection at the Cr K-edge was done by detuning of 50% the intensity of the incident beam which was measured by use of a He/Ne/air-filled ion chamber. At least five acquisitions were recorded for each sample, in the range 5900−6760 eV for Cr K-edge and 9550−10 500 eV for Zn K-edge at 2 eV/5 s, and then averaged before EXAFS extraction. For the Ge 7-elements data, care was taken to analyze each element data before summation for possibly not taking account of it. The possible evolution within each sample was controlled by the comparison of the first and the last scan at both edges: no change has been noted. Between each measure, samples were kept in a refrigerator; scans at interval of 24 h did not reveal any modification of the EXAFS oscillations.

Data were treated by the same way, by use of the program package EXAFS pour le MAC.[18] The normalized EXAFS function was obtained from the Lengeler−Eisenberger formula, with a linear model for the preedge background, and the postedge absorption reproduced by a cubic spline polynomial function. The E_o edge energy was taken as 5990 eV for Cr K-edge and 9664 eV for Zn K-edge. The EXAFS signal, $\chi(k)$, was k^3-weighted and Fourier-transformed throughout a Kaiser window on the range spectrum 4.0−13.5 Å^{-1} for Cr data ($\tau = 2.5$) and 3.4−12.5 Å^{-1} for Zn data ($\tau = 3.0$). The program ROUND MIDNIGHT was used for fitting procedures, and the reliability of the fit was given by the value of the residual factor, defined as

$$\rho = \sum_i k_i[\chi_{\exp}(k_i) - \chi_{th}(k_i)]^2 \Big/ \sum_i k\chi_{\exp}(k_i)^2$$

Phase and amplitude functions for the absorbing and backscatterer (Cr,O) pair were extracted from the filtering of the first peak of the EXAFS Fourier transform of $Cr(NO_3)_3 \cdot 9H_2O$, where the chromium absorbing atom is surrounded by 6 O at 1.96 Å,[19] with an electron reduction factor $S_0^2 = 1$, a parameter $\Gamma = 0$ related to the mean free path, and a Debye−Waller factor $\sigma = 0.07$ Å. For the absorbing and backscatterer (Cr,Cr) pair, phase and amplitude functions were extracted from the filtering of the second peak of the EXAFS Fourier transform of $ZnCr_2O_4$, attributed mainly[20] to 6 Cr at 2.94 Å, with $S_0^2 = 1$, $\Gamma = 0$, and $\sigma = 0.06$ Å. EXAFS refinement with these backscattering functions were made by considering an energy shift ΔE equal to 0. For the absorbing and backscatterer (Zn,O) pair, reference compounds encountered in the literature all exhibit distortion in the oxygen octahedra, so we used theoretical phase and amplitude functions generated by FeFF6[21] considering a cluster ZnO_6, which were calibrated for Γ and ΔE by fitting the first peak of the EXAFS Fourier transform of $Zn(NO_3)_2 \cdot 2H_2O$. Parameters of the fit were $S_0^2 = 1$, $N = 6$ (coordination number, fixed), $R = 2.06$ Å, $\sigma = 0.093$ Å, $\Gamma = 0.625$, and $\Delta E = 3.24$ eV for a residual factor $\rho = 0.5\%$.

Results

UV−Visible Spectroscopy. The UV−visible spectra recorded at different stages of the LDH formation are reported in Figure 1. The signature of the UV−visible spectra so obtained are gathered in Table 1. Until a volume $V = 7.5$ mL of added salts (Figure 1a), the spectra obtained are characterized by signatures of hydrolytic oligomers of Cr(III). These oligomeric species have been extensively studied by Stünzi and Marty,[16] and for comparison with the signatures observed in this work, the published results for the different oligomers are summarized in Table 2. As a matter of fact, the

(15) Boclair, J. W.; Braterman, P. S.; Jiang, J.; Lou, S.; Yarberry, F. *Chem. Mater.* **1999**, *11*, 303.
(16) Stünzi H.; Marty W. *Inorg. Chem.* **1983**, *22*, 2145.
(17) Jolivet, J. P. In *De la solution à l'oxyde*; InterEditions/CNRS Editions: Paris, 1994.
(18) Michalowicz, A. Thesis, Université Paris Val de Marne, 1990.
(19) Lazar, D.; Ribar, B.; Divjakovic, V.; Meszaros, C. *Acta Crystallogr.* **1991**, 1060.
(20) Roussel, H. Thesis, Université Blaise Pascal (Clermont-Ferrand), 1999.
(21) Rehr, J. J.; Mustre de Leon, J.; Zabinsky, S. I.; Albers, R. C. *J. Am. Chem. Soc.* **1991**, *113*, 5135.

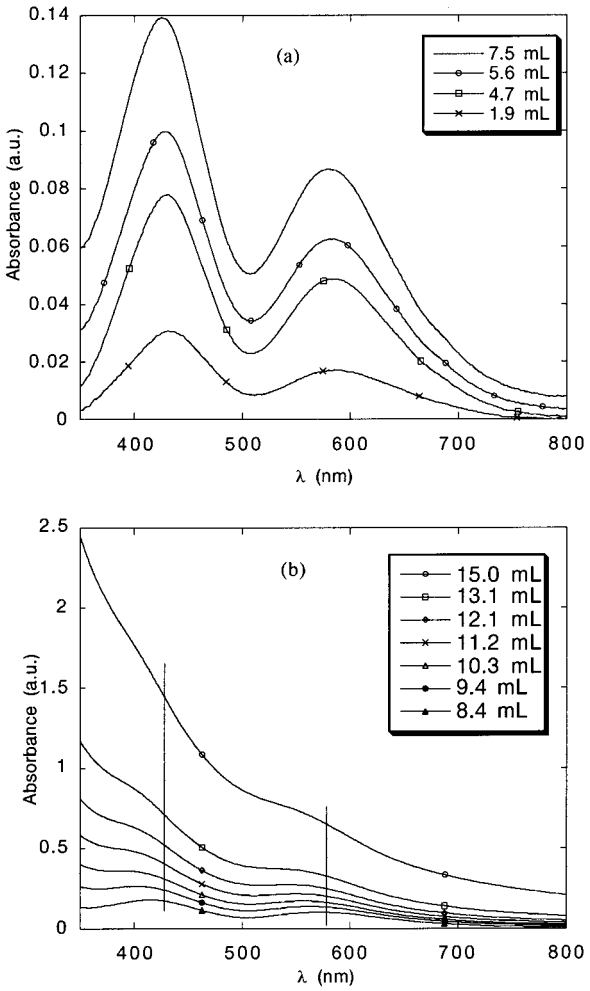

Figure 1. UV−Visible spectra for solutions with (a) less than 7.5 mL and (b) more than 8.4 mL of added Cr(III) and Zn(II) salts.

Table 1. Band Position within the UV−Visible Absorbance Spectra of Taken Solutions at Different Volumes of Salts Added

V (salts), mL added	λ_1, nm	λ_2, nm	$\alpha = \epsilon_{max1}/\epsilon_{max2}$
1.9	432	586	1.82
4.7	429	585	1.59
5.6	427	583	1.59
7.5	425	581	1.61
8.4	414	571	1.74
9.4	401	567	
10.3	391	563	
11.2	382	560	
12.1	376	556	
13.1	365	554	
15.0	348	544	

signature (432, 586, 1.82) for $V = 1.9$ mL agrees well with the one reported by Stünzi for deprotonated chromium(III) monomers $Cr(OH)(H_2O)_5^{2+}$ and $Cr(OH)_2(H_2O)_4^{+}$ (430, 590, 1.75). It is noteworthy that Stünzi reports the formation of such deprotonated monomers in the pH range 4.3−6.0, which is quite in the range of the synthesis condition used in this work (pH = 5.0). For sample corresponding to $V = 4.7$ mL of added salts, the signature (429, 585, 1.59) is intermediate between those of the deprotonated monomer and the Cr(III) trimer (425, 584, 1.60), indicating probably the coexistence of monomeric and trimeric oligomers at this stage of the condensation of Cr(III) cations. When the addition of salts goes further (for $V = 5.6$ mL), the preponderance of the trimeric species becomes more evident, with the signature (427, 583, 1.59). Finally, for $V = 7.5$ mL, the band positions (425, 581) are close to the ones reported by Stünzi and Marty[16] for the tetrameric species (426, 580), but the measured ratio α (1.61) between the maxima absorbance remains always close to that of the trimeric species, which strongly suggests the presence of both oligomers.

Table 2. Band Positions within the UV−Visible Absorbance Spectra of the Different Hydrolytic Oligomers Cr(III) Reported in the Literature[16]

oligomeric species	λ_1, nm	λ_2, nm	$\alpha = \epsilon_{max1}/\epsilon_{max2}$
$Cr(H_2O)_6^{3+}$	408	575	1.17
$Cr(OH)(H_2O)_5^{2+}$	430	590	1.75
$Cr(OH)_2(H_2O)_4^{+}$	430	590	1.75
$Cr_2(OH)_2(H_2O)_8^{4+}$	417	582	1.18
$Cr_3(OH)_4(H_2O)_9^{5+}$	425	584	1.60
$Cr_4(OH)_6(H_2O)_{10}^{6+}$	426	580	1.95
$Cr_4(OH)_6(H_2O)_{11}^{6+}$	426	580	1.95
$Cr_4O(OH)_5(H_2O)_{10}^{5+}$	426	580	1.95

Sampling made on solutions with more than 8.4 mL of added salts (Figure 1b) presents absorbance bands (Table 1) that are not typical of oligomeric species. Del Arco et al.[22] report as characteristic wavelengths of solid LDH phase [Co−Cr−CO_3] 405 and 540 nm, whereas Labajos and Rives[23] have found for solid LDHs [Mg−Cr−CO_3] and [Ni−Cr−CO_3] the maxima wavenumbers (400, 570) and (385, 580) nm, respectively. We can assume in this present work that the signatures observed for more than $V = 8.4$ mL of added salts indicate the incorporation of Cr(III) cations in the LDH sheets.

To verify the possible presence of oligomeric species at the advanced stages of the addition of the mixed solution, we have characterized the supernatant liquid obtained after ultracentrifugation. First, it appears that at this stage of reaction ≈80% of chromium ions introduced in the solution are incorporated into the LDH solid. Second, the ≈20% of chromium ions remaining in the solution are characterized by UV−visible signature (425, 582, 1.42) corresponding to a mixture of trimeric/tetrameric species.

EXAFS. The EXAFS spectra at both K-edges for each sample as a function of the volume of added salts are reported in Figure 2 and compared to the signal of the final LDH. Obvious changes can be observed at the *k* values marked by lines in Figure 2, which are fingerprints of the LDH phase. These changes in the EXAFS spectra are strongly revealed in the pseudoradial distribution functions (PRDFs) (uncorrected for phase shifts) presented in Figure 3. In both cases, the first peak located at ≈1.7 Å in the PRDF is related to the first coordination shell of six oxygen atoms in an octahedral environment. Simulations indicate no change in the M−O distance of the first coordination shell during the synthesis: the average distance is 1.96 ± 0.02 and 2.06 ± 0.02 Å for Cr−O and Zn−O, respectively. Beyond the first coordination shell of oxygen atoms, we can note a distinct evolution of the local order around each cation.

(22) del Arco, M.; Galiano, M. V. G.; Rives, V.; Trujillano, R.; Malet, P. *Inorg. Chem.* **1996**, *35*, 6362.
(23) Labajos, F. M.; Rives, V. *Inorg. Chem.* **1996**, *35*, 5313.

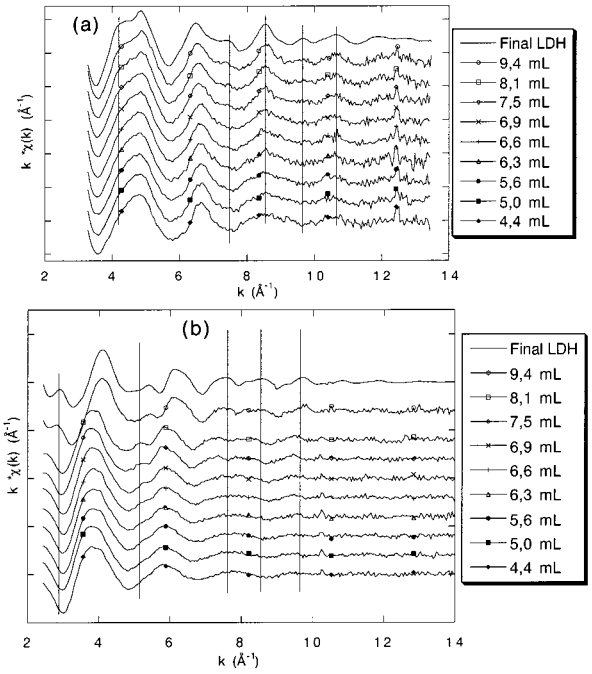

Figure 2. EXAFS spectra recorded (a) at the Cr K-edge and (b) at the Zn K-edge for different solutions taken during the synthesis.

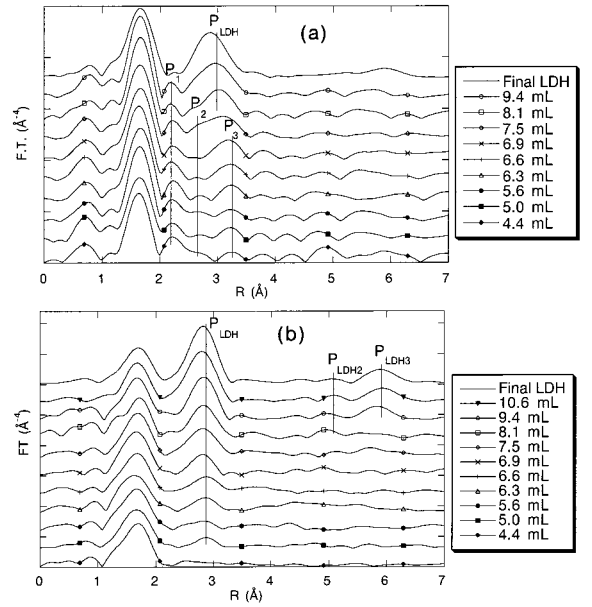

Figure 3. Modulus of the PRDF of EXAFS signal recorded (a) at the Cr K-edge and (b) at the Zn K-edge for different solutions taken during the synthesis.

Results obtained at the Zn K-edge (Figure 3b) show clearly a limit in concentration of salts added in solution, above which the formation of LDH phase is observed. The PRDF of sample corresponding to $V = 4.4$ mL of mixed salts added in solution shows only the peak related to the first oxygen coordination shell, indicating that zinc atoms form the hexaaquo complex $Zn(H_2O)_6^{2+}$. As soon as a volume $V = 5.0$ mL of salts is added in the reactor, the appearance of the peak labeled P_{LDH}, which corresponds to the first metallic neighbors at 3.11 Å in the final LDH compound [Zn−Cr−Cl],[24] evidences the

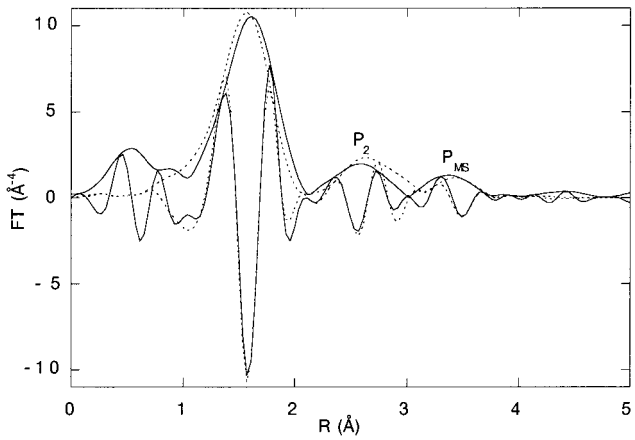

Figure 4. Modulus of the PRDF of EXAFS signal (solid line) recorded for a solution of 0.1 M Cr(III) with a hydrolysis ratio $h = 1.5$ and its simulation (dashed line) with a Cr dimer and the FeFF6 code.

incorporation of Zn atoms in the LDH phase. Finally, we can note on the PRDFs of the two last samples ($V =$ 9.4 and 10.6 mL) the significative presence of the peaks P_{LDH2} and P_{LDH3}, corresponding to the metallic neighbors located from the absorbing atom at $\sqrt{3}a$ ($a = 3.11$ Å is the distance M−M) and $2a$, respectively,[24] in the LDH solid phase.

For Cr K-edge (Figure 3a), the typical peak P_{LDH} of the first metallic neighbors in the final LDH solid[24] which indicates the incorporation of Cr(III) in the LDH sheets, is evident on the PRDFs recorded only for more than 7.5 mL of added salts. At the early stages of the synthesis, the medium-range order around chromium is characterized by three peaks noted P_1, P_2, and P_3 observed between 2 and 3.5 Å. As similar contributions are not observed at the Zn K-edge and due to the evidence by UV−visible spectroscopy of chromium oligomers at these stages of salts addition, we must attribute the P_1, P_2, and P_3 peaks either to Cr−Cr contributions in Cr(III) oligomeric species or to multiple scattering contributions inside oligomers. Due to the mixture of oligomeric species in solution, we tried for identification to obtain solutions with a single type of oligomers. This has been done only for dimers.

Dimers have been obtained predominantly by addition of NaOH to a 0.1 M aqueous solution of $CrCl_3 \cdot 6H_2O$ with a hydrolysis ratio $h = [OH^-]/[Cr^{3+}] = 1.5$. In this case, the measured UV−visible fingerprint was (417, 580, 1.28), which is very close to the fingerprint reported in Table 2 for dimer. The PRDF of such dimers is presented in Figure 4 together with the calculated signal issued from an FeFF6 simulation taking into account as dimer a model in which two distorted octahedra are sharing a common edge. This model is build from the crystallographic structure of $(H_2O)_4Cr(\mu\text{-}OH)_2Cr(H_2O)_4^{4+}$ cation,[25] in which the O−Cr−O angle involving the two bridging hydroxo groups is 78.2°. This reported distortion is responsible to a lengthening of the Cr−Cr distance in adjacent edge sharing octahedra from 2.78 Å (ideal octahedra with angles equal to 90°) to 3.00 Å in the crystal. Accordingly, the fitting parameters obtained from the simulation presented in Figure 4 for

(24) Roussel, H.; Briois, V.; Elkaïm, E.; de Roy, A.; Besse, J. P. *J. Phys. Chem. B* **2000**, *104*, 5915.

(25) Spiccia, L.; Stoeckli-Evans, H.; Marty, W.; Giovanoli, R. *Inorg. Chem.* **1987**, *26*, 474.

the first and second peaks are six oxygen atoms at 1.96 Å and one chromium atom at 2.99 Å, respectively. The third peak of the PRDF is identified as originating from multiple scattering processes inside the octahedron as reported in ref 26. The comparison between the PRDFs of Figure 3a and the PRDF of dimers in Figure 4 allows us to identify peak P_2 as a contribution of chromium atoms at a distance from the central absorbing atom of 2.99−3.00 Å in edge-sharing octahedra.

Peak P_1 is located at a shorter distance than peak P_2. It has been first tentatively assigned to chlorine contribution in the first coordination shell. Chlorine amplitude and phase functions were extracted from the FeFF code and checked on the anhydrous $CrCl_3$ solid[27] for which six chlorine atoms are located at 2.368 Å. On one hand, the resulting fit of the filtered signal in the PRDF located between 1 and 2.5 Å considering oxygen and chlorine atoms in the first coordination shell gave a poor agreement with the experimental signal. On the other hand, such a mixed oxygen/chlorine first coordination shell does not account for the UV−visible results, since it is reported in the literature[28] that such a mixed coordination shell gives rise to bands around 475 and 665 nm for the $Cr[Cl_3(H_2O)_3]$ unit, 450 and 635 nm for the $Cr[Cl_2(H_2O)_4]$ unit, and 430 and 605 nm for the $Cr[Cl(H_2O)_5]$ unit. Furthermore, it is reported in the literature[28] that such $[CrCl_n(H_2O)_{6-n}]^{(3-n)+}$ complexes are formed in very acidic media (pH <1 obtained by dissolution of $CrCl_3 \cdot 6H_2O$ in concentrated HCl solution). At pH = 5, which is the pH value used herein for the LDH synthesis, and in diluted media in chloride ions (chloride ions are only coming from the addition of $CrCl_3$ and $ZnCl_2$ salts), the presence of chloride ions in the first coordination shell of chromium is very unlikely. This hypothesis was consequently refuted. The peak P_1 is located at too short a distance from the absorbing atom to be considered as related to multiple scattering processes. Then the only suitable interpretation for this peak is a contribution of chromium atoms at $R < 2.98$ Å.

A drawback of the EXAFS analysis within the single scattering approximation compared to the analysis of XRD data is that determination of distances alone (even accurately) is not sufficiently constraining to rebuild a unique structural model. The EXAFS technique often needs the assistance of other techniques to propose a satisfactory structural model. As previously mentioned, the UV−visible results require for interpretation consideration of structural models involving trimers and tetramers in the composition of the mixture of oligomers in solution. It is important to know if the structures of oligomers are in agreement with the EXAFS results. According to the Stünzi published results,[16] one trimer and three tetramers such as those presented in Figure 5 can be considered. The models result from the condensation of distorted octahedra like those involved in the formation of dimers.[17] In addition to the distance of 2.98 Å between chromium atoms, we find in these

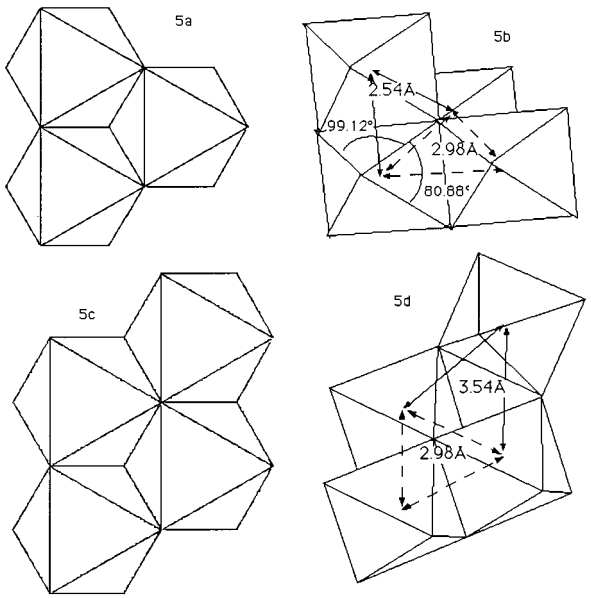

Figure 5. Different Cr(III) oligomers according to the Stünzi published results.[16]

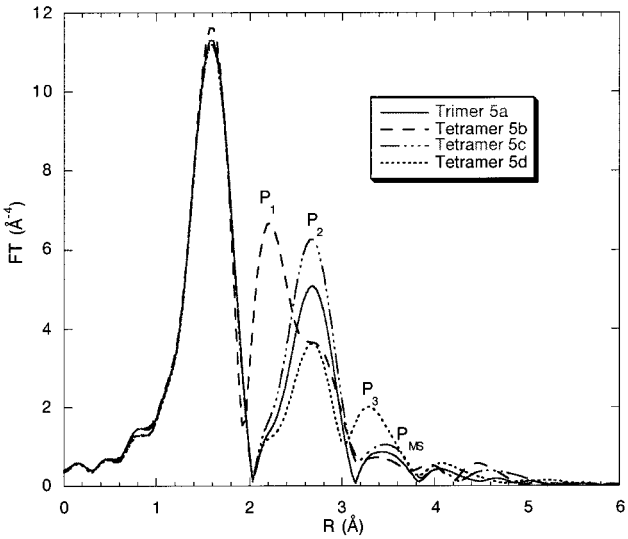

Figure 6. Modulus of the PRDF of ab initio EXAFS signal obtained for the oligomers displayed in Figure 5 with the FeFF6 code in the multiple scattering framework.

models a short Cr−Cr distance at 2.54 Å for skewed tetramers (model 5b) and a long Cr−Cr distance at 3.54 Å for double corner tetramers (model 5d). These short and long distances result from the angular distortion in the octahedra previously mentioned. It is important to note that the tetramer displayed in Figure 5d with a two-shared-corner octahedron has been already reported by Jones et al.[29] but with a longer distance Cr−Cr of 3.65 Å, whereas a short Cr−Cr distance at 2.55 Å has been reported in the $[(NH_3)_3Cr(OH)_3Cr(NH_3)_3](I_3)_2I$ compound.[30] The different models have been separately simulated by FeFF6 and the corresponding results are presented in Figure 6. We note that the PRDF of the skewed tetramer (model 5b) presents peaks in the positions of P_1 and P_2 and that the one of the double-

(26) Sakane, H.; Munoz-Paez, A.; Diaz-Moreno, S.; Martinez, J. M.; Pappalardo, R. R.; Sanchez Marcos, E. *J. Am. Chem. Soc.* **1998**, *120*, 10401.

(27) Wyckoff, R. W. G. *Crystal Structures*, 2nd ed.; Interscience Publishers: New York, 1964; Vol. 2.

(28) Diaz-Moreno, S.; Munoz-Paez, A.; Martinez, J. M.; Pappalardo, R. R.; Sanchez Marcos, E. *J. Am. Chem. Soc.* **1996**, *118*, 12654.

(29) Jones, D. J.; Roziere, J.; Maireles-Torres, P.; Jimenez-Lopez, A.; Oliveira-Pastor, P.; Rodriguez-Castellon, E.; Tomlinson, A. A. G. *Inorg. Chem.* **1995**, *34*, 4611.

(30) Tebbe, K. F.; Gilles, T. *Z. Naturforsch.* **1998**, *53b*, 1127.

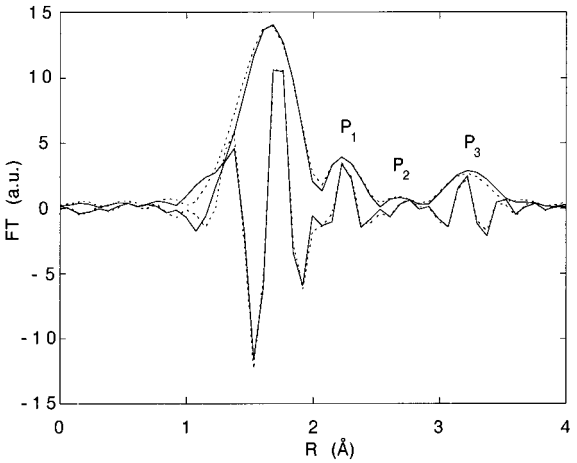

Figure 7. Simulation (dashed line) of the four first peaks of the PRDF of the EXAFS signal (solid line) recorded for the solution V (salts) = 6.3 mL [$\Delta E = 0$, $\Gamma = 0$ for all shells; $\sigma =$ 0.06 (fixed) for P_1, P_2, and P_3 ; $N_1 = 0.6$, $N_2 = 0.3$, and $N_3 =$ 1.2; $R_1 = 2.54$, $R_2 = 2.99$, and $R_3 = 3.48$ Å; reliability factor 2.8%].

corner tetramer (model 5d) presents peaks in the positions of P_2 and P_3. All these simulations were performed with the inclusion of multiple scattering processes in the cluster, taking into account a global Debye−Waller factor of 0.063 Å for scattering paths beyond the first coordination shell. As evidenced previously for the dimer (Figure 4), but also for the trimer (5a), the skewed tetramer (5b), and the planar tetramer (5c), multiple scattering events begin to contribute only above peak P_2 with a peak centered around 3.45 Å and labeled P_{MS}. This result can make critical the assignation of peak P_3. Nevertheless, we can observe in Figure 6 that the single scattering contribution by one chromium atom at 3.54 Å in the tetramer 5d giving rise to the peak P_3 is faintly located at a shorter distance (3.25 Å) than the peak P_{MS}. In fact, as displayed in Figure 7 for the sample with 6.3 mL of added salts, satisfactory agreement in the fit is obtained for the simulation of the PRDF in the R range between 1 and 4 Å by considering oxygen contribution at 1.96 ± 0.02 Å and chromium contributions at 2.54 ± 0.02, 2.99± 0.02, and 3.48 ± 0.02 Å. Fits on the other samples extracted from the reactor with $V < 7.5$ mL have given similar results, making the structures presented in Figure 5 valid models to take into account for both the EXAFS and UV−visible results.

As clearly evidenced at the Zn K-edge, the amplitude of the P_{LDH} peak increases with the added salts volume. This result is also verified at the Cr K-edge for solutions with more than 7.5 mL of added salts. This result can be interpreted by an increase of the LDH solid proportion in the mixture of hexaaquo and oligomeric species and of the LDH phase. But it can also be due to an increase in size of the nanometer-sized LDH solid phase, which would induce in the PRDF an increase of mean coordination numbers for second and higher shells. To solve this problem, ultracentrifuged solutions have been studied corresponding to 6.9, 7.5, and 10.6 mL of added salts. Solids collected for the three samples show the characteristic purple color of the final LDH, and their respective EXAFS spectra are quite similar to the final LDH at both cation K-edges, as reported in Figure 8 for sample issued from a solution with 6.9 mL of added

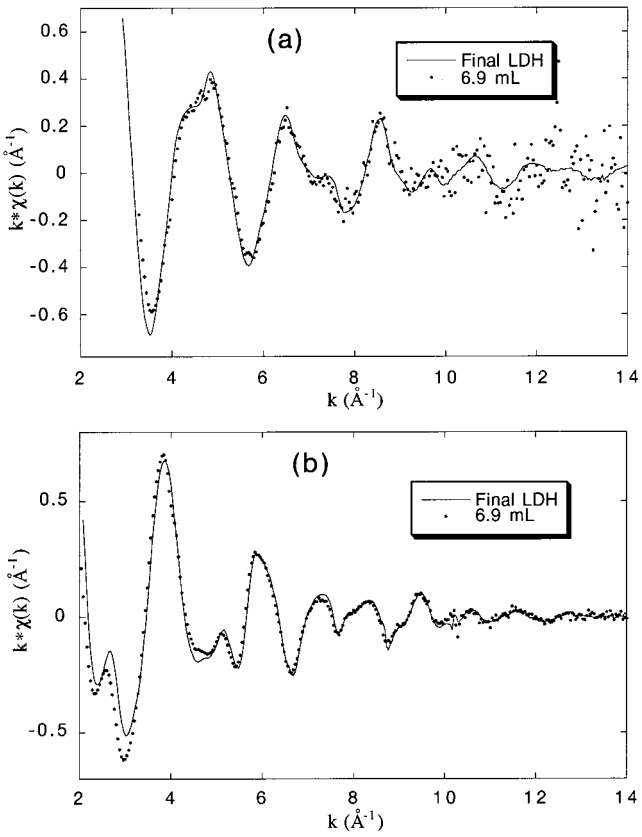

Figure 8. EXAFS spectra (a) at the Cr K-edge and (b) at the Zn K-edge of final LDH (solid line) and solid (dotted line) collected after ultracentrifugation of solution with V (salts) = 6.9 mL.

salts. The crystallite sizes of the LDH [Zn-Cr-Cl] determined from XRD[24] are of about 400−500 Å along the stacking of the sheets and of more than 2000 Å in the plane of the brucite-like sheets. The argument of the formation of nanocrystalline LDH powders with increasing size to explain the increase in the amplitude of the P_{LDH} peak does not hold. The PRDFs associated with the supernatant liquid collected after ultracentrifugation confirm the UV−visible results. We observe in Figure 9a in the PRDFs recorded at the Cr K-edge the three peaks, P_1, P_2, and P_3, attributed previously to Cr−Cr contributions in oligomeric species. For 10.6 mL of added salts, the peak P_1 is more intense than for the other solutions, suggesting the presence of the skewed tetramer (Figure 5b) in a higher concentration at the end of the reaction than at the early stages. At the Zn K-edge, the PRDFs reported in Figure 9b are typical of the hexaaquo complex $Zn(H_2O)_6^{2+}$, with only one coordination shell, as for the first sample studied [V(salts) = 4.4 mL].

Discussion

As the [Zn−Cr−Cl] LDH phase appears in solution—i.e., for at least 5.0 mL of added salts—EXAFS results clearly evidence the coexistence of the solid LDH phase with oligomeric chromium(III) species and hexaaquozinc-(II) complexes. From linear combinations of the EXAFS spectra of the final solid LDH and of the supernatant solution obtained after ultracentrifugation (for example, $V = 6.9$ mL), the EXAFS spectra of each sample at both cation K-edges can be reproduced and the proportion of

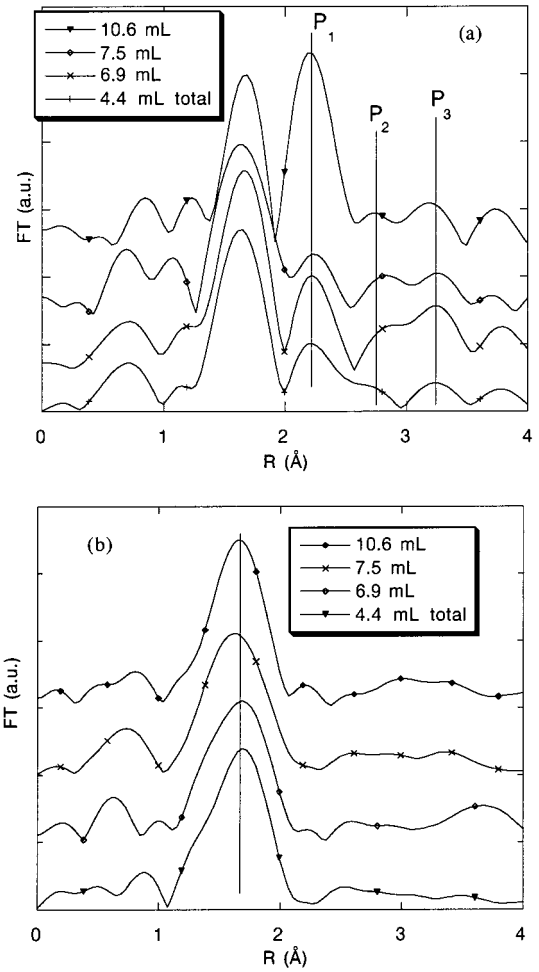

Figure 9. Moduli of the EXAFS Fourier transform (a) at the Cr K-edge and (b) at the Zn K-edge for supernatant solutions obtained by ultracentrifugation, compared to the modulus of the EXAFS Fourier transform of the sample obtained for $V =$ 4.4 mL of added salts.

Table 3. Proportion of Metal Incorporated in LDH[a]

V (salts) (mL)	Cr	Zn
4.4	0	0
5.0	10	5
5.6	10	10
6.3	20	15
6.6	25	18
6.9	25	25
7.5	50	50
8.1	65	60
9.4	75	80

[a] Calculated from the linear combination of spectra of final LDH and liquid after ultracentrifugation reproducing the total solutions spectra.

cations in solid or oligomeric states is then known. The combination results for both cations are reported in Table 3 and an example of such simulation is given in Figure 10 at both cation K-edges. The good reproduction of the experimental EXAFS spectra in this way validates our method. Table 3 shows that the proportions of Cr and Zn incorporated in the LDH sheets are quite similar during the synthesis, which means that the cations nominally introduced in the reactor with a ratio Zn:Cr = 2:1 constitute the LDH sheets in the same ratio. This result eliminates the possibility of a cationic

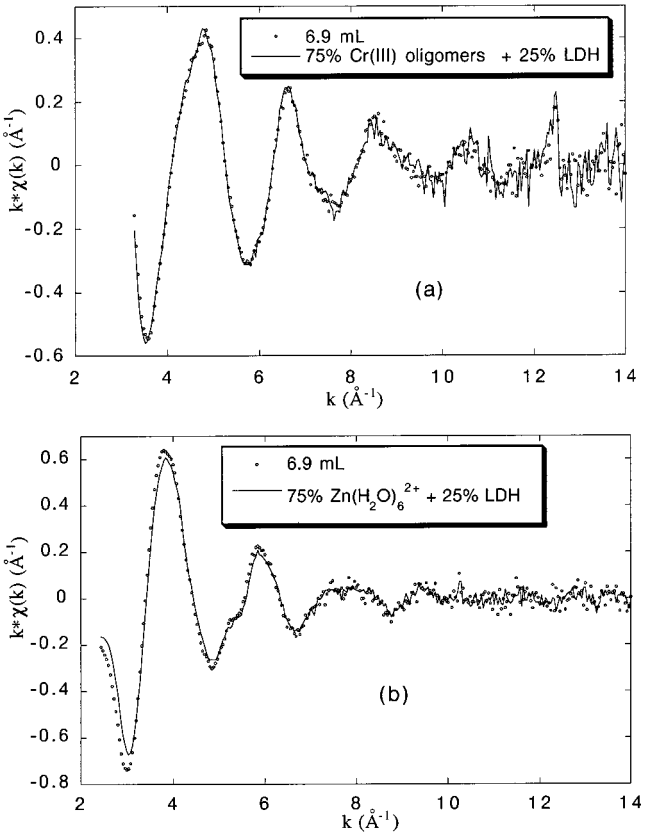

Figure 10. Rebuilt EXAFS spectra by linear combination of spectra of final LDH and supernatant solution after ultracentrifugation for the solution V (salts) = 6.9 mL (a) at the Cr K-edge and (b) at the Zn K-edge.

segregation within the LDH sheets, i.e., an area containing only one of the cations.

Our experimental conditions proceed by constant addition of chromium and zinc salts in solution maintained at pH = 5.0. So, as observed by Boclair and Braterman,[9] the formation of the [Zn−Cr−Cl] LDH phase occurs by a one-step process, excluding the initial precipitation of trihydroxide followed by LDH formation as for systems involving other trivalent ions, Al or Fe, for instance. Due to structural results obtained in this work, we propose in the following a structural pathway for condensation of Cr(III) and Zn(II) into LDH sheets.

The chromium(III) ion is well-known to be strongly inert with respect to condensation reactions and to form slowly Cr(III) oligomers in acid conditions.[17,31] UV−Visible and EXAFS spectroscopy show clearly the formation of trimeric and tetrameric chromium(III) species at the early stages of addition of salts in solution. At pH = 5.0, the deprotonated Cr(III) complexes, $Cr(OH)(H_2O)_5^{2+}$ and $Cr(OH)_2(H_2O)_4^{+}$ evidenced by UV−visible spectroscopy after addition of 1.9 mL of salts, are the common precursors of all these oligomers formed by olation reactions involving nucleophilic substitutions of water molecules by hydroxo ligands between hydroxylated complexes of Cr(III).[17]

Besides the formation of oligomeric chromium species, we have shown by EXAFS the existence of hexaaquozinc complexes at the early stages of the synthesis ($V =$ 4.4

(31) Henry, M.; Jolivet, J. P.; Livage, J. *Structure and Bonding*; Springer-Verlag: Berlin, 1990.

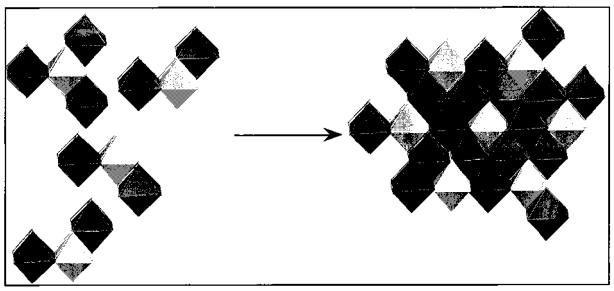

Figure 11. Proposed pathway for the formation of the [Zn-Cr-Cl] sheets.

mL). At pH = 5.0, these aquo complexes cannot condense and form oligomeric species because they are not hydrolyzed. Until the Zn(II) cations are inserted into the LDH sheets, they remain in the hexahydrated complex form.

In fact, as the formation of oligomeric species of Cr(III) is slow, the competitive formation of mixed complexes Zn−Cr is possible because the water molecules in the coordination shell of Zn(II) ions are labile and the hydroxylated chromium(III) complexes have OH groups with a strong nucleophilic character. Then Cr−OH−Zn bridges can be formed according to reaction 1 corresponding to the global stoichiometry OH/(Cr + 2Zn) = 6:

$$Cr(OH)_x(H_2O)_{6-x}^{(3-x)+} + 2Zn(H_2O)_6^{2+} + (6-x)OH^- \leftrightarrow Zn_2(\mu_2\text{-}OH)_4Cr(OH)_x(H_2O)_8^{+} + (10-x)H_2O \quad (1)$$

Further condensation between these mixed complexes can proceed by elimination of coordinated water to zinc moieties and formation of μ_3-OH bridges leading to the positively charged sheets $[Zn_2Cr(OH)_6^+]$ of the LDH phase.

According to these reactions, a schematic structural pathway for the formation of the LDH compound is presented in Figure 11. This pathway strongly supports the concept of cationic order in the [Zn−Cr−Cl] LDH sheets suggested by de Roy et al.[11] and Hofmeister and Platen[13] but not demonstrated until now. By this way, a Cr center is necessarily surrounded by six Zn centers, explaining why the ratio Zn:Cr = 2:1 is always obtained for [Zn−Cr−Cl] LDH. Two explanations can be pointed out to explain the difficulty encountered in proving the cationic ordering in such phases. On one hand, we have already shown in a previous work[24] that the expected intensity of the peaks of superstructure relative to the order within the layers is close to 0.1% of the maximum intensity obtained for the (*003*) reflections. Then, such reflections are very difficult to detect by XRD. On the other hand, we cannot discard some faults in the ordering scheme due to inclusion of Cr(III) oligomeric species in the LDH sheets. Indeed some species such as the trimer (model 5a) or the planar tetramer[17] (model 5c) could incorporate the LDH sheets by OH-bridging with the Zn complexes by the same way as the monomer units. But it is important to note that in such a case the ratio Zn:Cr found would be less than 2, as shown by Gutmann and Muller[12] for insertion of dimer units under particular synthesis conditions. Such a ratio less than 2 has never been observed for the coprecipitation

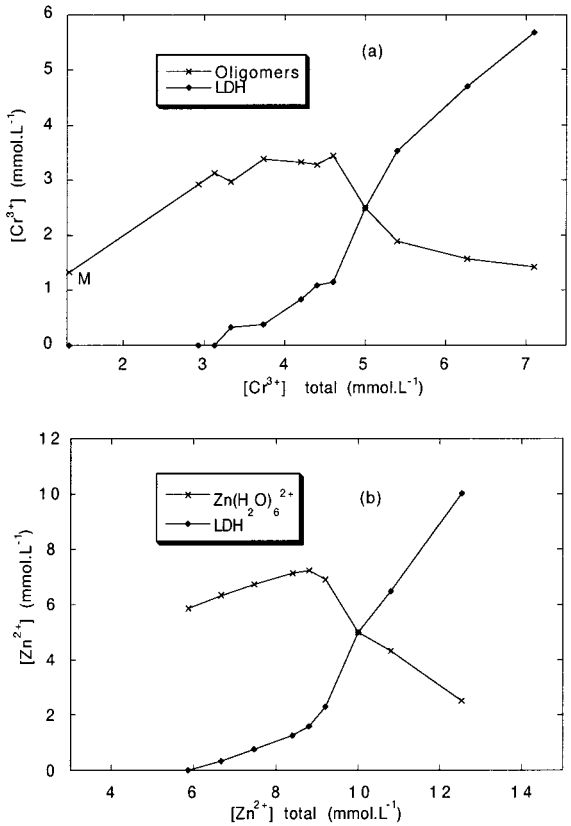

Figure 12. Proportion of oligomeric species and LDH phase as a function of total amount of cation introduced in solution (a) for Cr(III) and (b) for Zn(II). These results are deduced from the linear combination of EXAFS spectra of final LDH and supernatant solution after ultracentrifugation.

conditions used in this work. Consequently, we can assume that such faults in ordering are exceptional. Dimeric, trimeric, and planar tetrameric species have more probably a role to play in the LDH formation by releasing in solution monomeric species. Namely, the chemical equilibria supporting the formation of oligomers, like reaction 2 proposed by Stünzi and Marty,[16]

$$Cr(OH)_2(H_2O)_4^{+} + Cr_3(OH)_6(H_2O)_9^{5+} \leftrightarrow Cr_4(OH)_6(H_2O)_{10}^{6+} + 3H_2O \quad (2)$$

can be displaced toward the release in solution of monomers to compensate the decrease of monomer concentration due to its incorporation into the LDH sheets.

As a matter of fact, the proportion of oligomeric species with respect to the LDH phase as a function of the total amount of chromium in solution decreases at the advanced stages of the reaction as displayed in Figure 12. Furthermore, for the last ultracentrifuged sample, which corresponds to 10.6 mL of added salts, EXAFS results have clearly shown the increase of the intensity of peak P_1. Full analysis of the corresponding EXAFS data are shown in Figure 13 and structural parameters are gathered in Table 4. The increase of the coordination number for the chromium atom at 2.54 Å at the advanced stages of the reaction can be interpreted as the predominant presence of the skewed tetramer displayed in Figure 5b in the mixture of oligomers characterizing the solution. This results for this tet-

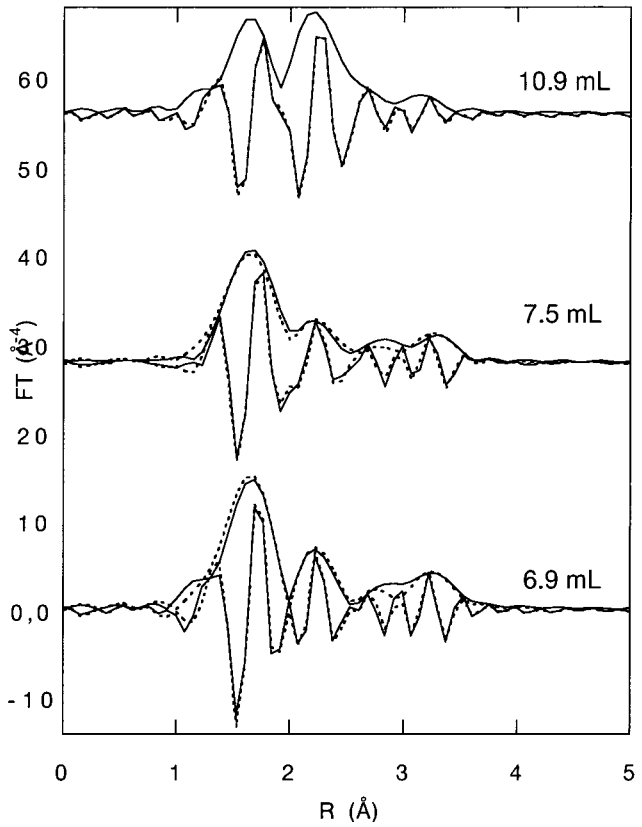

Figure 13. Simulation (dashed line) of the four first peaks of the PRDF of the EXAFS signal (solid line) recorded at the Cr K-edge for the three supernatant solutions obtained by ultracentrifugation. Structural parameters are gathered in Table 4.

ramer from the irreversible formation of a μ_3-oxo bridge hindering possible displacement of equilibria like reaction 2 toward the release of monomers. Tetramers modeled in Figure 5b are a dead-end route for the formation of the LDH phase.

Conclusion

The cations Cr(III) clearly plays a key role during the formation of the sheets of the [Zn−Cr−Cl] LDH because the hydroxylated complexes are inert toward substitution and condensation reactions. Although trimers and tetramers of Cr(III) are formed at the pH of the synthesis (pH = 5.0) as evidenced by EXAFS and UV−visible spectroscopy at the early stages of reaction, heterocondensation between hexaaquozinc(II) complexes and deprotonated chromium monomers seems to be the way leading to the formation of LDH phase in which Cr cations are always surrounded by six Zn cations. This structural pathway is totally in agreement with cationic order suggested by several authors for the [Zn−Cr−Cl] LDH because of the fixed ratio Zn:Cr = 2. Nevertheless, although this must be very exceptional, we cannot discard some faults in the ordering scheme due to addition of Cr(III) oligomeric species (dimer, trimer, or planar tetramer) in the LDH sheets.

Table 4. Structural Parameters of the Simulation of the Filtered EXAFS Signal[a]

	6.9 mL	7.5 mL	10.6 mL
oxygen number	6.0	6.0	6.0
σ (Å)	0.05	0.06	0.07
R (Å)	1.95	1.96	1.98
chromium number	0.8	1.2	1.8
σ (Å)	0.01	0.07	0.03
R (Å)	2.56	2.54	2.53
chromium number	0.5	0.5	1.1
σ (Å)	0.1	0.05	0.03
R (Å)	3.00	3.00	2.95
chromium number	1.0	0.9	0.8
σ (Å)	0.01	0.03	0.06
R (Å)	3.54	3.55	3.49
reliability factor (%)	3.0	4.4	1.0

[a] Ranging from 1 to 4 Å in the PRDF displayed in Figure 13 for supernatant solutions obtained by ultracentrifugation.

Acknowledgment. We thank F. Villain and F. Bouamrane for use of the UV−visible spectrometer, technical assistance in the chemistry lab, and constant development of equipment around EXAFS experiments. Fernando Palomo is acknowledged for providing electronic system to regulate pH during synthesis.

CM001066W